Vectorial Wave Analysis of Inhomogeneous Optical Fibers Using Finite Element Method

KATSUNARI OKAMOTO AND TAKANORI OKOSHI, MEMBER, IEEE

Abstract—**A vectorial wave analysis of the propagation characteristics of radially inhomogeneous optical fibers is presented. The vectorial wave equation is first translated into a variational problem, and then it is solved by using the finite element method. The results are compared with those of the scalar wave analysis. The error caused by the scalar wave approximation is discussed for wide variety of refractive index profiles. It is shown that the error caused by the scalar wave approximation is about 0.1 percent for eigenvalues and 1 percent for delay time, when the relative index difference between core and cladding is 1 percent.**

I. Introduction

In the analysis of transmission characteristics of optical fibers, the scalar wave approximation is often made because it simplifies the analysis remarkably whereas the resulting error is tolerable in most cases. To obtain the estimate of the error, however, the result of the analysis must be compared with that of rigorous (vectorial wave) analysis.

So far two methods of the vectorial wave analysis of inhomogeneous optical fibers (having arbitrary refractive-index profiles) have been presented: 1) one using the staircase approximation [1]–[5], and 2) the other using the direct numerical integration [6]–[8]. Among them one paper [2] showed the error caused by the scalar wave approximation, but only for quadratic index profiles.

This paper presents first a new method of the vectorial wave analysis of the propagation characteristics of inhomogeneous optical fibers using finite element method. In the latter half of this paper, results of the vectorial wave and scalar wave analyses are compared for a wide variety of refractive index profiles. It is shown that the errors caused by the scalar wave approximation in the eigenvalue and delay time are about 0.1 and 1 percent, respectively, when the relative index difference $\Delta = (n_1^2 - n_2^2)/2n_1^2 = 1$ percent, where n_1 and n_2 denote the maximum index in the core and the cladding index, respectively.

II. Variational Formulation

We first express the axial components of electric and magnetic fields as

$$E_z = (\omega^2 \varepsilon_1 \mu_0/\beta)\Phi(r) \cos(n\theta + \phi_n) \tag{1}$$

$$H_z = \omega \varepsilon_1 \Psi(r) \sin(n\theta + \phi_n),\ n\text{: integer},\ \phi_n = 0 \text{ or } \pi/2 \tag{2}$$

where ω denotes the angular frequency, ε_1 the maximum permittivity in the core, β the propagation constant, and n the rotational mode number. From Maxwell's equations, the following vectorial wave equations for $\Phi(r)$ and $\Psi(r)$ are obtained [9]:

$$\frac{1}{r}\frac{d}{dr}\left[\frac{(1-f)}{(\chi-f)} r \frac{d\Phi}{dr}\right] + \left[k^2 n_1^2 (\chi - f) - \frac{n^2}{r^2}\right] \cdot \frac{(1-f)}{(\chi-f)}\Phi + \frac{n}{r}(1-\chi)\Psi \frac{d}{dr}\left(\frac{1}{\chi-f}\right) = 0 \tag{3}$$

$$\frac{1}{r}\frac{d}{dr}\left[\frac{1}{(\chi-f)} r \frac{d\Psi}{dr}\right] + \left[k^2 n_1^2 (\chi - f) - \frac{n^2}{r^2}\right] \cdot \frac{1}{(\chi-f)}\Psi + \frac{n}{r}\Phi \frac{d}{dr}\left(\frac{1}{\chi-f}\right) = 0 \tag{4}$$

where

$$f(r) \triangleq 1 - \varepsilon(r)/\varepsilon_1 \tag{5}$$

$$\chi \triangleq 1 - \beta^2/\omega^2 \varepsilon_1 \mu_0. \tag{6}$$

From Maxwell's equations, the transverse components of electric and magnetic fields are also obtained; these are

$$E_r = -j\frac{1}{(\chi-f)}\left[\frac{d\Phi}{dr} + \frac{n}{r}\Psi\right]\cos(n\theta + \phi_n) \tag{7}$$

$$E_\theta = j\frac{1}{(\chi-f)}\left[\frac{d\Psi}{dr} + \frac{n}{r}\Phi\right]\sin(n\theta + \phi_n) \tag{8}$$

$$H_r = -j\frac{\beta}{\omega\mu_0}\cdot\frac{1}{(\chi-f)}\left[\frac{d\Psi}{dr} + \frac{(1-f)n}{(1-\chi)r}\Phi\right] \cdot \sin(n\theta + \phi_n) \tag{9}$$

$$H_\theta = -j\frac{\beta}{\omega\mu_0}\cdot\frac{1}{(\chi-f)}\left[\frac{(1-f)\,d\Phi}{(1-\chi)\,dr} + \frac{n}{r}\Psi\right] \cdot \cos(n\theta + \phi_n). \tag{10}$$

The solutions $\Phi(r)$ and $\Psi(r)$ which satisfy the above vectorial wave equations ((3) and (4)) and the boundary conditions (the continuity of E_z, H_z, E_θ, and H_θ at the core-cladding boundary: $r = a$) may also be obtained as that

Manuscript received April 14, 1977; revised June 1, 1977.

K. Okamoto was with the Department of Electronic Engineering, University of Tokyo, Bunkyo-ku, Tokyo 113, Japan. He is now with Nippon Telegraph and Telephone Public Corporation, Ibaraki Electrical Communication Laboratory, Tokai, Ibaraki, 319-11 Japan

T. Okoshi is with the Department of Electronic Engineering, University of Tokyo, Bunkyo-ku, Tokyo 113, Japan.

0018-9480/78/0200-0109$00.75

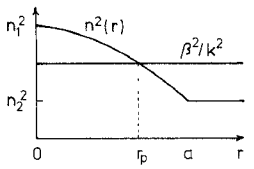

Fig. 1. Relation between the refractive index profile $n(r)$ and the normalized propagation constant β/k.

solution of the variational problem to make the following functional stationary (see Appendix I):

$$I[\Phi,\Psi] = \frac{1}{(1-\chi)}\int_0^a \frac{(1-f)}{(\chi-f)}\left[\left(\frac{d\Phi}{dr}\right)^2 + \frac{n^2}{r^2}\Phi^2\right] r\,dr - \frac{k^2 n_1^2}{(1-\chi)}\int_0^a (1-f)\Phi^2 r\,dr + \int_0^a \frac{1}{(\chi-f)} \cdot \left[\left(\frac{d\Psi}{dr}\right)^2 + \frac{n^2}{r^2}\Psi^2\right] r\,dr - k^2 n_1^2 \int_0^a \Psi^2 r\,dr + \int_0^a \frac{2n}{(\chi-f)}\frac{d}{dr}(\Phi\Psi)\,dr - \frac{1}{(\chi-2\Delta)} \cdot \left[\Omega_\beta \frac{(1-2\Delta)}{(1-\chi)}\Phi^2(a) + 2n\Phi(a)\Psi(a) + \Omega_\beta \Psi^2(a)\right] \tag{11}$$

where

$$w = (\beta^2 - k^2 n_2^2)^{1/2} a \tag{12}$$

$$\Omega_\beta = wK_n'(w)/K_n(w) \tag{13}$$

and K_n denotes the nth order modified Bessel function of the second kind.

III. Solution of the Variational Problem by Finite Element Method

To solve variational problems, the Rayleigh–Ritz method is most commonly used. (For the analysis of fibers, see [10] for example.) However, in the present case it cannot be used for the following reason. From (5) and (6),

$$(\chi - f) = \frac{[n^2(r) - \beta^2/k^2]}{n_1^2}. \tag{14}$$

Since β^2/k^2 varies in the range $n_1^2 < \beta^2/k_1^2 \le n^2$ for propagating modes, $(\chi - f)$ becomes zero at one point $(r = r_p)$ as shown in Fig. 1. The Rayleigh–Ritz method cannot be applied to the present problem because the term $(\chi - f)$ in the denominator of (11) becomes zero at $r = r_p$, where the integrand diverges.

This difficulty can be avoided by using the finite element method. We first divide the region between $r = 0$ and $r = a$ into N elements (see Fig. 2), and express the values of $\Phi(r)$ and $\Psi(r)$ at $r = r_l$ as

$$\Phi_l = \Phi(r_l), \qquad \Psi_l = \Psi(r_l), \qquad l = 0, 1, 2, \cdots, N. \tag{15}$$

Note that the division is made so that r_p coincides one of the

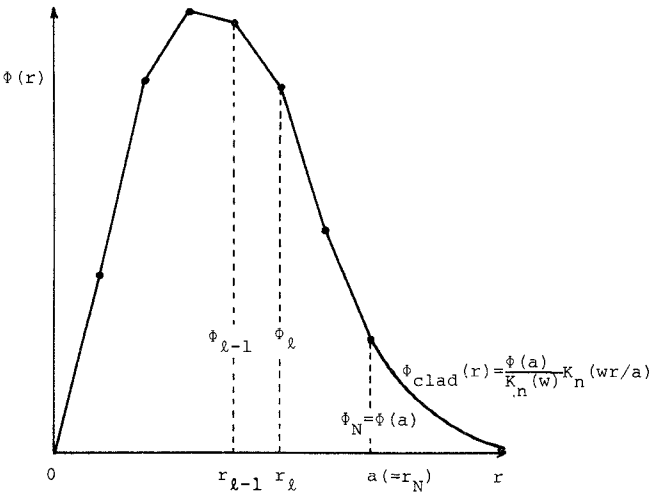

Fig. 2. Finite element representation of $\Phi(r)$.

r_l's. In each of these elements, functions $\Phi(r)$ and $\Psi(r)$ are expressed as

$$\Phi(r) = \Phi_{l-1}F_{l-1}(r) + \Phi_l F_l(r), \qquad r_{l-1} \le r \le r_l \tag{16}$$

$$\Psi(r) = \Psi_{l-1}F_{l-1}(r) + \Psi_l F_l(r), \tag{17}$$

where $F_{l-1}(r)$ and $F_l(r)$ are continuous functions of r satisfying the following conditions:

$$F_{l-1}(r_{l-1}) = 1, \qquad F_{l-1}(r_l) = 0$$
$$F_l(r_{l-1}) = 0, \qquad F_l(r_l) = 1. \tag{18}$$

In those elements which do not include the singular point $(r = r_p)$, the function $F_l(r)$'s are approximated, as is done in most finite element analyses [11], by linear functions as shown in Fig. 2. In those elements including r_p, to avoid the divergence of the integral, $\Phi(r)$ and $\Psi(r)$ are approximated as

$$\Phi(r) = (Ar^{-n} + Br^n) - (Cr^{-n} + Dr^n)(\chi - f)^2 \tag{19}$$

$$\Psi(r) = (Ar^{-n} - Br^n) - (Cr^{-n} - Dr^n)(\chi - f)^2 \tag{20}$$

where n is the rotational mode number, and constants A, B, C, D are determined so that $\Phi(r)$ and $\Psi(r)$ coincides with Φ_p and Ψ_p at $r = r_p$ and with Φ_{p-1} and Ψ_{p-1} at $r = r_{p-1}$, respectively.

To make the functional I stationary with respect to all the parameters Φ and Ψ, the following conditions must hold for all l:

$$\frac{\partial I}{\partial \Phi_l} = 0, \qquad \frac{\partial I}{\partial \Psi_l} = 0. \tag{21}$$

Substituting (16)–(20) into (11) and using the stationary conditions: (21), we obtain a matrix equation of the form

$$\begin{bmatrix} \boldsymbol{S} & \boldsymbol{T} \\ \boldsymbol{T} & \boldsymbol{P} \end{bmatrix} \begin{bmatrix} \Phi \\ \Psi \end{bmatrix} = 0 \tag{22}$$

where $\Phi = [\Phi_0, \Phi_1, \cdots, \Phi_N]^T$, $\Psi = [\Psi_0, \Psi_1, \cdots, \Psi_N]^T$, and $\boldsymbol{S}$, $\boldsymbol{T}$, $\boldsymbol{P}$ are $(N+1) \times (N+1)$ matrices whose elements are

given as follows. (For space limitations only significant elements are shown.)

$$S_{l,l-1} = -\frac{k^2 n_1^2}{(1-\chi)} \int_{r_{l-1}}^{r_l} (1-f) F_{l-1} F_l r \, dr + \frac{1}{(1-\chi)} \int_{r_{l-1}}^{r_l} \frac{(1-f)}{(\chi - f)} \cdot \left[\frac{dF_{l-1}}{dr} \frac{dF_l}{dr} + \frac{n^2}{r^2} F_{l-1} F_l \right] r \, dr \tag{23}$$

$$T_{l,l-1} = n \int_{r_{l-1}}^{r_l} \frac{1}{(\chi - f)} \frac{d}{dr} (F_{l-1} F_l) \, dr \tag{24}$$

$$P_{l,l-1} = -k^2 n_1^2 \int_{r_{l-1}}^{r_l} F_{l-1} F_l r \, dr + \int_{r_{l-1}}^{r_l} \frac{1}{(\chi - f)} \cdot \left[\frac{dF_{l-1}}{dr} \frac{dF_l}{dr} + \frac{n^2}{r^2} F_{l-1} F_l \right] r \, dr. \tag{25}$$

In order that a nontrivial solution of (22) exists,

$$\begin{vmatrix} \boldsymbol{S} & \boldsymbol{T} \\ \boldsymbol{T} & \boldsymbol{P} \end{vmatrix} = 0 \tag{26}$$

must hold. This equation is the rigorous eigenvalue (dispersion) equation which determines the propagation constants of an inhomogeneous optical fiber.

IV. Scalar Wave Approximation

Since for practical fibers χ and $|f(r)|$ are much smaller than unity, we may approximate in (3) and (4) as

$$1 - f(r) \doteqdot 1, \qquad 1 - \chi \doteqdot 1. \tag{27}$$

Under such approximations, as shown by Yamada and Inabe [12], adding (3) and (4) or subtracting (3) from (4), we may obtain the scalar wave equations (see Appendix II). If we put the scalar wave approximation (27) into (11), the functional may be simplified as

$$I[\Phi,\Psi] = \int_0^a \frac{1}{(\chi - f)} \left[\left(\frac{d\Phi}{dr} \right)^2 + \frac{n^2}{r^2} \Phi^2 \right] \cdot r \, dr - k^2 n_1^2 \int_0^a \Phi^2 r \, dr + \int_0^a \frac{1}{(\chi - f)} \left[\left(\frac{d\Psi}{dr} \right)^2 + \frac{n^2}{r^2} \Psi^2 \right] \cdot r \, dr - k^2 n_1^2 \int_0^a \Psi^2 r \, dr + \int_0^a \frac{2n}{(\chi - f)} \frac{d}{dr} (\Phi\Psi) r \, dr - \frac{1}{(\chi - 2\Delta)} \cdot [\Omega_\beta \Phi^2(a) + 2n\Phi(a)\Psi(a) + \Omega_\beta \Psi^2(a)]. \tag{28}$$

By solving the above variational problem by the aforementioned finite element method, we obtain the eigenvalue equation corresponding to (26) having a form

$$\begin{vmatrix} \boldsymbol{P} & \boldsymbol{T} \\ \boldsymbol{T} & \boldsymbol{P} \end{vmatrix} = 0. \tag{29}$$

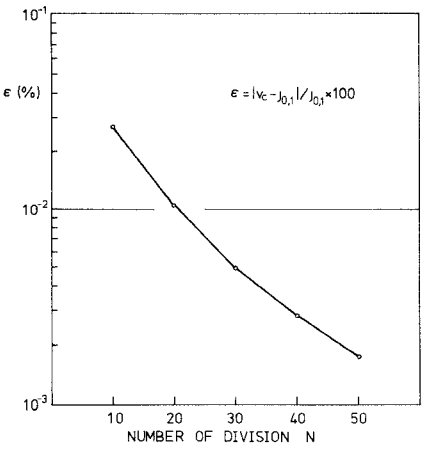

Fig. 3. The accuracy of the finite element method (FEM) versus the number of divisions. Parameter v_c is the normalized cutoff frequency of a uniform core fiber for the TE_{01}-mode obtained by the FEM, whereas $j_{0,1}$ (= 2.4048256 ···) is the exact solution.

This is the eigenvalue equation obtained with the scalar wave approximation.

V. Numerical Results

The accuracy of the finite element method analysis itself is first investigated. The normalized cutoff frequency v of the TE_{01}-mode in a uniform core fiber is computed by the finite element method, and compared with the exact value: $j_{0,1} = 2.4048256 \cdots$ [13]. The accuracy thus estimated is shown in Fig. 3 as a function of the number of divisions in the finite element method analysis.

Next, the error caused by the scalar wave approximation is investigated by comparing the results of analyses using (26) and (29). For this purpose we consider index profiles given as

$$n^2(r) = n_1^2[1 - 2\rho\Delta(r/a)^\alpha], \qquad 0 \le r \le a \tag{30}$$

where ρ is a parameter representing the presence of step or valley at core-cladding boundary. Examples of the profiles expressed by (30) are shown in Fig. 4.

Fig. 5(a) and (b) shows the error in the eigenvalue (normalized frequency v) caused by the scalar wave approximation as functions of α and ρ, respectively.[1] The term "error in the eigenvalue" requires comments. In the present estimation of the error, for the sake of convenience, the errors (difference between solutions of (26) and (29)) in the eigenvalues (the normalized frequency v) which give three specific propagation constants β for the TM_{01}-mode are computed first.[2] The specific propagation constants are

[1] One might doubt why the error in v is plotted instead of that in β (or x). It is simply because the error appears in such a form that the v–x curve is translated in the horizontal direction (parallel to the v-axis), without changing its overall shape remarkably. (In such a case the error in β (or x) is strongly dependent upon $d\beta/dv$ (or dx/dv) and hence upon v.) Besides, the estimation of error in terms of v is better consistent with that of $d\beta/d\omega$ (see Fig. 7).

[2] The estimation of error for higher order modes is left for further study.

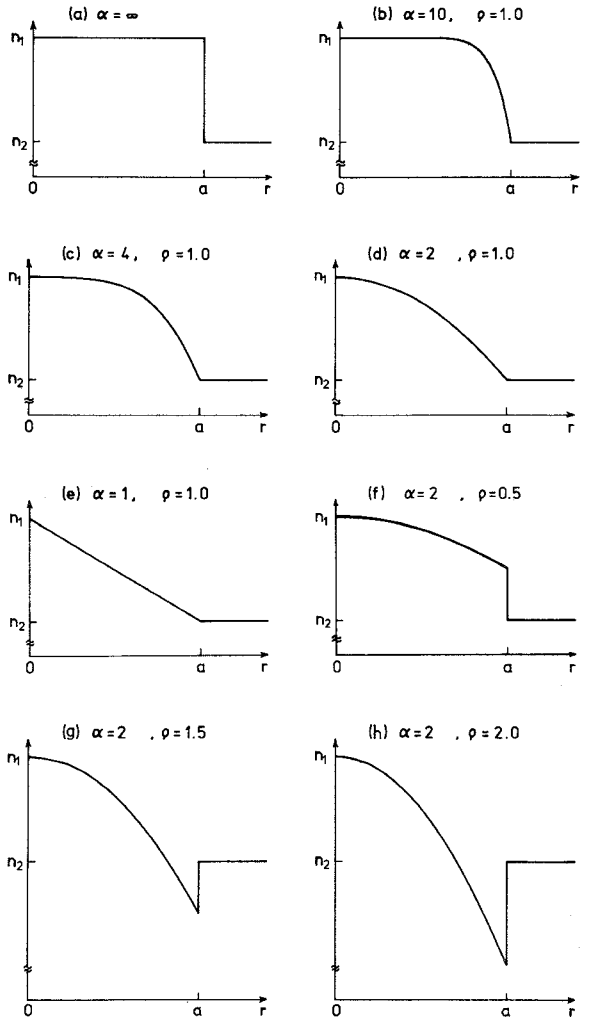

Fig. 4. Examples of refractive index profiles used in the numerical analyses.

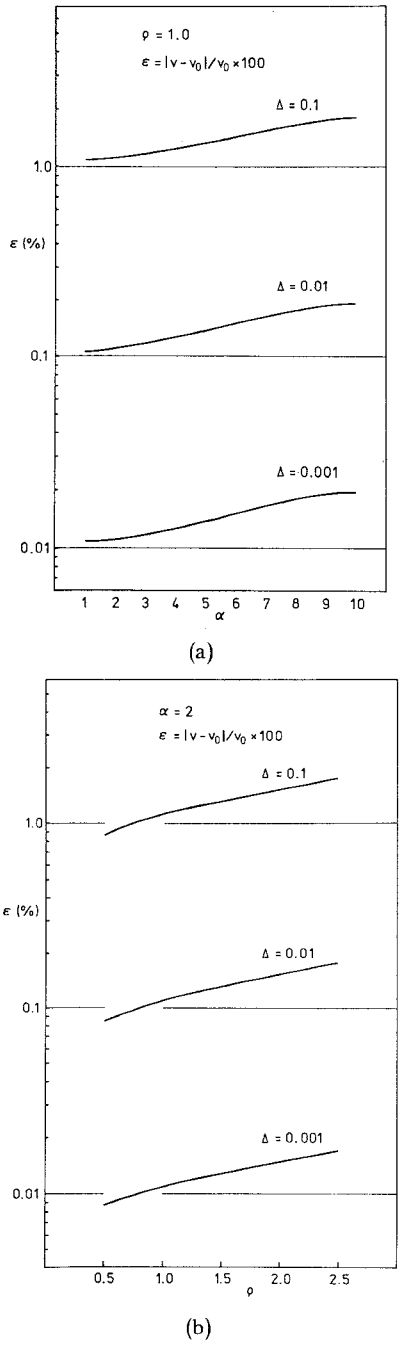

Fig. 5. Error in the eigenvalue caused by the scalar wave approximation: (a) Functions of α. (b) Functions of ρ.

chosen as $x = 0.25$, 0.50, and 0.75 where x is a normalized parameter defined as

$$x = \frac{n_1^2 - (\beta/k)^2}{n_1^2 - n_2^2}. \tag{31}$$

The computed errors are then averaged for the three points to obtain ε shown in the ordinate of Fig. 5(a) and (b). It is found that when $\Delta = 1$ percent, which is the typical index difference in multimode fibers, the error caused by the scalar wave approximation is of the order of magnitude of 0.1 percent.

Next, the error caused by the scalar wave approximation in the group delay is estimated. As a preliminary step, we first compute the exact group delay by using the vectorial wave analysis. Fig. 6 shows the exact normalized delay difference defined by

$$D = \left| \frac{c}{n_1} \frac{d\beta}{d\omega} - 1 \right|, \qquad c\text{: light velocity} \tag{32}$$

as a function of the exponent α, for the TM_{01} mode at a frequency where $x = 0.3$. Note that D is a parameter proportional to the delay difference between the TM_{01}-mode and a fictitious wave having velocity equal to n_1/c (see the ordinate in the right of Fig. 6). It is found in Fig. 6 that the delay difference is reduced remarkably (to about 1 ns/km) at $\alpha = 2$; this is a well-known fact [14].

Next the difference between the rigorous value of D and that computed upon the scalar wave approximation was computed; the result is shown in Fig. 7 for $\Delta = 10$, 1, and 0.1 percent as functions of α. When $\Delta = 1$ percent, the error is approximately 0.01 ns/km for $\alpha = 2$ (1 percent of D), and 0.8 ns/km for $\alpha = 10$ (6 percent of D). Note that the percentage

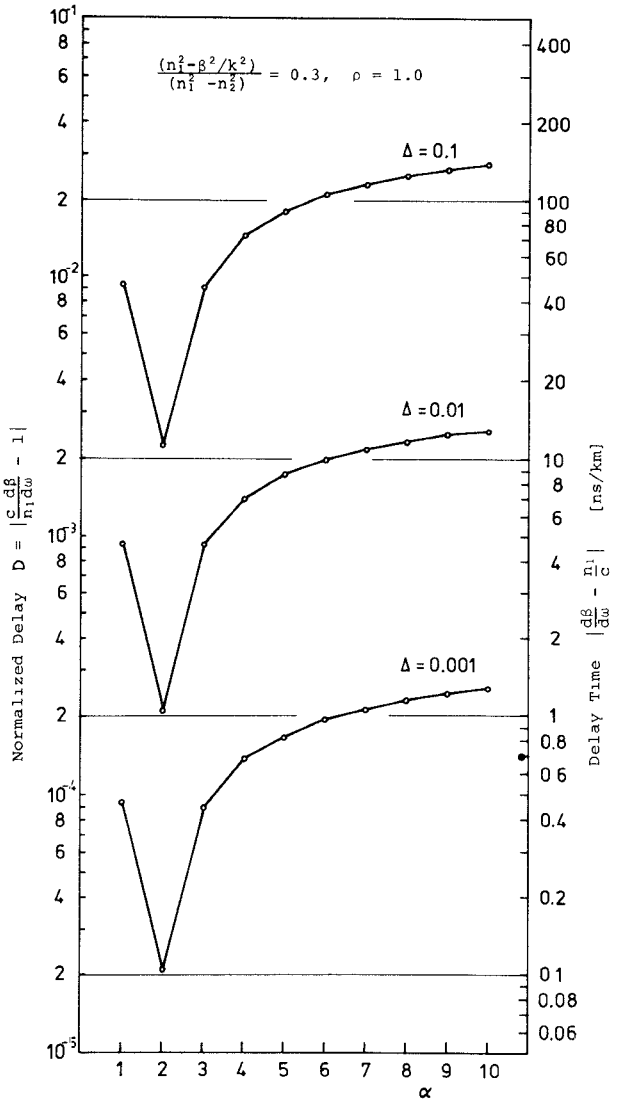

Fig. 6. Variation of the delay time for various exponents α and $\rho = 1.0$, at $x = 0.3$ (exact solution). $n_1 = 1.5$.

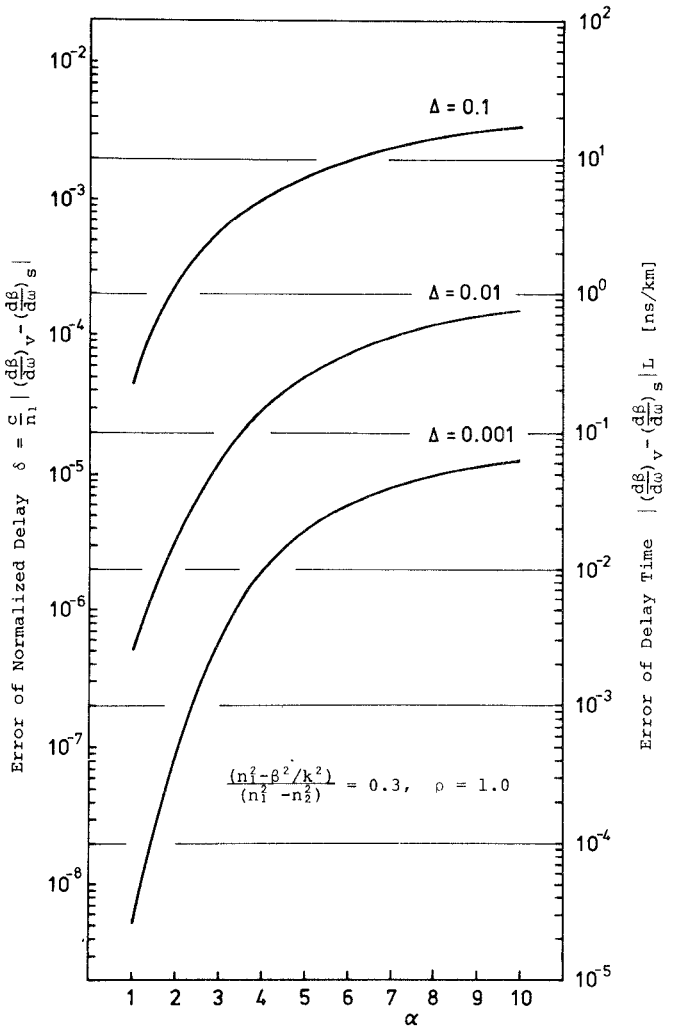

Fig. 7. Error in the delay time caused by the scalar wave approximation for $\rho = 1.0$, at $x = 0.3$. Derivatives $(d\beta/d\omega)_v$ and $(d\beta/d\omega)_s$ denote the delay time per unit length obtained by the vectorial wave and scalar wave analyses, respectively $n_1 = 1.5$.

error in the delay difference is much larger than that in the eigenvalues.

VI. Conclusion

Vectorial wave analysis of propagation characteristics of multimode optical fibers has been performed, and the error caused by the scalar wave approximation has been estimated. It has been found that the error in the eigenvalues is tolerable, whereas that in the group delay difference is relatively large.

Appendix I
Proof of the Validity of the Functional (11)

We assume that $I[\Phi,\Psi]$ is stationary for $\Phi = \Phi_0$ and $\Psi = \Psi_0$, and consider slightly deviated functions

$$\Phi(r) = \Phi_0(r) + \delta \cdot \eta(r) \tag{A.1}$$

$$\Psi(r) = \Psi_0(r) + \delta \cdot \zeta(r) \tag{A.2}$$

where $\eta(r)$ and $\zeta(r)$ are arbitrary continuous functions of r, and δ denotes a small real quantity. Putting the above $\Phi(r)$ and $\Psi(r)$ into (11) and assuming that $I[\Phi,\Psi]$ is stationary for $\delta = 0$, we obtain

$$\begin{aligned}\frac{1}{2}\cdot\frac{\partial I}{\partial\delta}\bigg|_{\delta=0} &= \frac{1}{(1-\chi)}\int_0^a \frac{(1-f)}{(\chi-f)}\left[\frac{d\Phi_0}{dr}\frac{d\eta}{dr}+\frac{n^2}{r^2}\Phi_0\eta\right] r\,dr \\ &\quad - \frac{k^2n_1^2}{(1-\chi)}\int_0^a (1-f)\Phi_0\eta r\,dr + \int_0^a \frac{1}{(\chi-f)} \\ &\quad \cdot \left[\frac{d\Psi_0}{dr}\frac{d\zeta}{dr}+\frac{n^2}{r^2}\Psi_0\zeta\right] r\,dr - k^2n_1^2\int_0^a \Psi_0\zeta r\,dr \\ &\quad + \int_0^a \frac{n}{(\chi-f)}\frac{d}{dr}(\Phi_0\zeta+\Psi_0\eta)\,dr - \frac{1}{(\chi-2\Delta)} \\ &\quad \cdot \left[\Omega_\beta\frac{(1-2\Delta)}{(1-\chi)}\Phi_0(a)\eta(a) + n\Phi_0(a)\zeta(a)\right. \\ &\quad \left. + n\Psi_0(a)\eta(a) + \Omega_\beta\Psi_0(a)\zeta(a)\right] = 0. \end{aligned} \tag{A.3}$$

By partial integration, (A.3) may be rewritten as

$$\begin{aligned}\frac{1}{2}\cdot\frac{\partial I}{\partial\delta}\bigg|_{\delta=0} = &-\int_0^a \frac{\eta(r)}{(1-\chi)}\left\{\frac{1}{r}\frac{d}{dr}\left[\frac{(1-f)}{(\chi-f)}r\frac{d\Phi_0}{dr}\right]\right.\\ &+\left[k^2n_1^2(\chi-f)-\frac{n^2}{r^2}\right]\frac{(1-f)}{(\chi-f)}\Phi_0\\ &\left.+\frac{n}{r}(1-\chi)\Psi_0\frac{d}{dr}\left(\frac{1}{\chi-f}\right)\right\}r\,dr\\ &-\int_0^a \zeta(r)\left\{\frac{1}{r}\frac{d}{dr}\left[\frac{1}{(\chi-f)}r\frac{d\Psi_0}{dr}\right]\right.\\ &+\left[k^2n_1^2(\chi-f)-\frac{n^2}{r^2}\right]\frac{1}{(\chi-f)}\Psi_0\\ &\left.+\frac{n}{r}\Phi_0\frac{d}{dr}\left(\frac{1}{\chi-f}\right)\right\}r\,dr\\ &+a\eta(a)\left\{\frac{1}{(\chi-f(a))}\left[\frac{(1-f)\,d\Phi_0}{(1-\chi)\,dr}+\frac{n}{r}\Psi_0\right]_{r=a}\right.\\ &\left.-\frac{1}{(\chi-2\Delta)}\left[\frac{(1-2\Delta)}{(1-\chi)}\frac{\Omega_\beta}{a}\Phi_0(a)+\frac{n}{a}\Psi_0(a)\right]\right\}\\ &+a\zeta(a)\left\{\frac{1}{(\chi-f(a))}\left[\frac{d\Psi_0}{dr}+\frac{n}{r}\Phi_0\right]_{r=a}\right.\\ &\left.-\frac{1}{(\chi-2\Delta)}\left[\frac{\Omega_\beta}{a}\Psi_0(a)+\frac{n}{a}\Phi_0(a)\right]\right\}. \qquad \text{(A.4)}\end{aligned}$$

Since $\eta(r)$ and $\zeta(r)$ are arbitrary functions of r, this equation shows that $\Phi_0(r)$ and $\Psi_0(r)$ satisfy the vectorial wave equations to be solved (3) and (4) and the boundary conditions at $r=a$:

$$\begin{aligned}&\frac{1}{(\chi-f(a))}\left[\frac{d\Psi_0}{dr}+\frac{n}{r}\Phi_0\right]_{r=a}\\ &\qquad=\frac{1}{(\chi-2\Delta)}\left[\frac{\Omega_\beta}{a}\Psi_0(a)+\frac{n}{a}\Phi_0(a)\right] \qquad \text{(A.5)}\\ &\frac{1}{(\chi-f(a))}\left[\frac{(1-f)\,d\Phi_0}{(1-\chi)\,dr}+\frac{n}{r}\Psi_0\right]_{r=a}\\ &\qquad=\frac{1}{(\chi-2\Delta)}\left[\frac{(1-2\Delta)}{(1-\chi)}\frac{\Omega_\beta}{a}\Phi_0(a)+\frac{n}{a}\Psi_0(a)\right] \qquad \text{(A.6)}\end{aligned}$$

which give the continuity of the electric and magnetic fields, respectively. (The left-hand sides of (A.5) and (A.6) express the fields in the core at $r=a$ (see (8) and (9)). The right-hand sides express those in the cladding.)

Appendix II
Proof that (27) Gives the Scalar Wave Equations

We first put the scalar wave approximation (27) into (3) and (4). Then, addition and subtraction of these equations yield

$$\begin{aligned}&\frac{1}{r}\frac{d}{dr}\left[\frac{1}{(\chi-f)}r\frac{d\Phi}{dr}\right]+\left[k^2n_1^2(\chi-f)-\frac{n^2}{r^2}\right]\\ &\qquad\cdot\frac{1}{(\chi-f)}\phi+\frac{n}{r}\phi\frac{d}{dr}\left(\frac{1}{\chi-f}\right)=0 \qquad \text{(A.7)}\end{aligned}$$

$$\begin{aligned}&\frac{1}{r}\frac{d}{dr}\left[\frac{1}{(\chi-f)}r\frac{d\psi}{dr}\right]+\left[k^2n_1^2(\chi-f)-\frac{n^2}{r^2}\right]\\ &\qquad\cdot\frac{1}{(\chi-f)}\psi-\frac{n}{r}\psi\frac{d}{dr}\left(\frac{1}{\chi-f}\right)=0 \qquad \text{(A.8)}\end{aligned}$$

where

$$\phi(r)=[\Phi(r)+\Psi(r)]/2 \qquad \text{(A.9)}$$

$$\psi(r)=[\Phi(r)-\Psi(r)]/2. \qquad \text{(A.10)}$$

Next we introduce transverse field functions $R_{HE}(r)$ and $R_{EH}(r)$ defined as

$$R_{HE}(r)=\frac{1}{(\chi-f)}\left[\frac{d\phi}{dr}+\frac{n}{r}\phi\right] \qquad \text{(A.11)}$$

$$R_{EH}(r)=\frac{1}{(\chi-f)}\left[\frac{d\psi}{dr}-\frac{n}{r}\psi\right]. \qquad \text{(A.12)}$$

Substituting (A.11) into (A.7) and (A.12) into (A.8), we obtain

$$\frac{1}{r}\frac{d}{dr}\left(r\frac{dR_{HE}}{dr}\right)+\left[k^2n_1^2(\chi-f)-\frac{(n-1)^2}{r^2}\right]R_{HE}=0 \qquad \text{(A.13)}$$

$$\frac{1}{r}\frac{d}{dr}\left(r\frac{dR_{EH}}{dr}\right)+\left[k^2n_1^2(\chi-f)-\frac{(n+1)^2}{r^2}\right]R_{EH}=0 \qquad \text{(A.14)}$$

which are known as the scalar wave equations.

References

[1] P. J B. Clarricoats and K. B. Chan, "Electromagnetic-wave propagation along radially inhomogeneous dielectric cylinders," *Electron Lett.*, vol. 6, no. 22, pp. 694–695, Oct 1970.

[2] T. Tanaka and Y Suematsu, "Matrix analysis of cylindrical fibers having arbitrary refractive-index distribution," Report of Technical Group on Optical and Quantum Electronics, OQE75-26, June 23, 1975

[3] ——, "An exact analysis of cylindrical fiber with index distribution by matrix method and its application to focusing fiber," *Trans. Inst Electron Commun. Eng. Japan*, vol. 59-E, no. 11, pp. 1–8, Nov 1976.

[4] E. Bianciardi and V Rizzoli, "Propagation in graded-core fibers A unified numerical description," *Opt. Quantum Electron.*, vol. 9, pp. 121–133, 1977.

[5] C. Yeh and G. Lindgren, "Computing the propagation characteristics of radially stratified fibers: An efficient method," *Appl. Opt*, vol. 16, no. 2, pp. 483–493, Feb. 1977.

[6] J G Dil and H. Blok, "Propagation of electromagnetic surface waves in a radially inhomogeneous optical waveguide," *Opto-Electron.*, vol. 5, pp. 415–428, 1973

[7] M. O. Vassell, "Calculation of propagating modes in a graded-index optical fiber," *Opto-Electron.*, vol. 6, pp 271–286, 1974.

[8] G. L. Yip and Y. H. Ahmew, "Propagation characteristics of radially inhomogeneous optical fiber," *Electron. Lett.*, vol. 10, pp. 37–38, Feb. 1974.

[9] C. N. Kurtz and W. Streifer, "Guided waves in inhomogeneous focusing media, Part I: Formulation, solution for quadratic inhomogeneity," *IEEE Trans. Microwave Theory Tech.*, vol. MTT-17, no. 1, pp. 11–15, Jan. 1969.

[10] T. Okoshi and K. Okamoto, "Analysis of wave propagation in inhomogeneous optical fibers using a variational method," *IEEE Trans. Microwave Theory Tech.*, vol. MTT-22, no. 11, pp. 938–945, Nov. 1974.

[11] O C. Zienkiewicz and Y. K. Cheung, *The Finite-Element Method in Continuous Structural Mechanics*. New York: McGraw-Hill, 1967.

[12] R. Yamada and Y. Inabe, "Guided waves along graded index dielectric rod," *IEEE Trans. Microwave Theory Tech.*, vol. MTT-22, no. 8, pp. 813–814, Aug. 1974.

[13] E. Snitzer, "Cylindrical dielectric waveguide modes," *J.O.S.A.*, vol. 51, no. 5, pp. 491–498, May 1961.

[14] D. Gloge and E. A. J. Marcatili, "Multimode theory of graded-core fibers," *Bell Syst. Tech. J.*, vol. 52, no 9, pp. 1563–1578, Nov. 1973.